Icarus **141**, 354–366 (1999)
Article ID icar.1999.6177, available online at http://www.idealibrary.com on IDEAL®

Cometary Evidence of a Massive Body in the Outer Oort Cloud

J. J. Matese,[1] P. G. Whitman, and D. P. Whitmire

Department of Physics, University of Louisiana at Lafayette, Lafayette, Louisiana, 70504-4210
E-mail: matese@usl.edu

Received September 9, 1998; revised March 11, 1999

Approximately 25% of the 82 new class I Oort cloud comets have an anomalous distribution of orbital elements that can best be understood if there exists a bound perturber in the outer Oort cloud. Statistically significant correlated anomalies include aphelia directions, energies, perihelion distances, and signatures of the angular momentum change due to the Galaxy. The perturber, acting in concert with the galactic tide, causes these comets to enter the loss cylinder—an interval of Oort cloud comet perihelion distances in the planetary region which is emptied by interactions with Saturn and Jupiter. More concisely, the impulse serves to smear the loss cylinder boundary inward along the track of the perturber. Thus it is easier for the galactic tide to make these comets observable. A smaller number of comets are directly injected by the impulsive mechanism. We estimate that the perturber–comet interactions take place at a mean distance of ≈25,000 AU. The putative brown dwarf would have a mass of $3 \overset{\times}{\div} 2 M_{\text{Jupiter}}$ and an orbit whose normal direction is within 5° of the galactic midplane. This object would not have been detected in the IRAS database, but will be detectable in the next generation of planet/brown dwarf searches, including SIRTF. It is also possible that its radio emissions would make it distinguishable in sensitive radio telescopes such as the VLA.

Key Words: **comets, dynamics; celestial mechanics; infrared observations; jovian planets.**

1. INTRODUCTION

Dominance of the galactic tide in making Oort cloud comets observable has been firmly established. Beginning with the work of Byl (1983), a succession of studies (see Matese and Whitman (1992) for a review of early contributions) has demonstrated that the distribution of orbital elements correlates well with the predictions of a theory that the adiabatic galactic disk tide is predominantly responsible for changing comet perihelia and bringing them into the observable zone. This is true during the present epoch and is likely to be true when averaged over long time scales (Heisler 1990).

The outer Oort cloud is formally defined as the interval of original cometary semimajor axes $\geq 10^4$ AU (Oort 1950). It has been shown that the vast majority of these comets are first-time entrants into the inner planetary region (Fernandez 1981) and are therefore commonly refered to as *new*. We denote the original value of semimajor axis, prior to perturbation by the planets, as A. More conveniently we discuss scaled original orbital energies $x \equiv 10^6$ AU/A so that the range of interest is $x \leq 100$. Accurate determination of the original energies of near-parabolic comets is made more difficult by observational uncertainties and outgassing. However, these effects do not substantively influence the determination of other orbital elements. The data we consider consists of those 82 new comets whose original energies have been calculated with sufficient accuracy to be deemed class I by Marsden and Williams (1996). Young comets with $x > 100$ provide only indirect evidence about the outer Oort cloud. New comets with less accurately known energies (class II) are less likely to be truly first-time entrants from the outer Oort cloud and are omitted since they could bias the analysis.

Our analysis is based on the data listed in Table I. It contains the relevant orbital elements of all 82 new class I comets. All angles refer to the galactic coordinate system and include the latitude, B, and longitude, L, of aphelia as well as an orientation coordinate of the angular momentum vector discussed below. They were obtained by us using standard transformations from ecliptic coordinates (Marsden and Williams 1996) to galactic coordinates. The scaled energy and perihelion distance are also listed.

In Fig. 1 we show the scatter in aphelia directions. We identify an anomalously abundant "great circle" of comet aphelia centered on galactic longitude 135°(315°) ±15°. A histogram summarizing the galactic longitude distribution is shown in Fig. 2. The fundamental question to be addressed is whether it is possible to identify dynamical signatures from the data.

Mechanisms considered include impulsive events from Oort-cloud-penetrating stars, tidal impulses from Oort-cloud-grazing molecular clouds, the adiabatic galactic interaction (both disk and core tides), and impulses from a putative bound perturber. In contrast to these dynamical options there is the chance that small-number statistics and observational selection effects preclude the possibility of identifying dynamical effects. Aphelia directional distributions in ecliptic, equatorial, and galactic coordinates have been studied (Matese *et al.* 1998), and it was concluded there that asymmetries in the observed distributions are unlikely to be entirely attributable to nondynamical explanations.

[1] To whom correspondence should be addressed. Fax: (318) 482-6699.

0019-1035/99 $30.00

TABLE I
New Class I Comets

Out of the great circle								In the great circle							
Comet		q (AU)	x	α (°)	L (°)	B (°)	$\dot{H}$	Comet		q (AU)	x	α (°)	L (°)	B (°)	$\dot{H}$
C/1890	F1	1.91	89	167.3	235.8	−23.7	−	C/1958	R1	1.63	76	134.0	307.7	−18.8	−
C/1955	G1	4.50	82	169.0	233.3	−29.4	−	C/1959	X1	1.25	69	66.4	124.3	−78.5	+
C/1941	K1	0.87	78	80.8	271.9	−35.1	+	C/1898	L1	1.70	68	314.9	143.9	28.8	−
C/1973	W1	3.84	71	63.3	32.7	48.2	−	C/1987	F1	3.62	59	185.8	130.4	−26.2	−
C/1972	L1	4.28	69	67.2	235.3	−39.9	+	C/1976	D2	6.88	59	315.0	121.8	−44.2	+
C/1937	C1	1.73	62	354.6	214.7	−38.7	+	C/1900	B1	1.33	57	264.6	305.5	42.1	+
C/1993	F1	5.90	59	214.2	330.2	−45.5	−	C/1989	Y1	1.57	49	96.5	329.2	−6.6	−
C/1973	A1	2.51	49	219.9	107.3	−50.6	−	C/1983	O1	3.32	48	356.1	325.3	54.7	−
C/1886	T1	0.66	46	314.4	288.7	−24.5	+	C/1888	R1	1.81	48	290.0	314.9	59.2	−
C/1987	H1	5.46	46	161.5	191.2	−17.0	−	C/1932	M2	2.31	45	171.7	146.9	−14.1	−
C/1912	R1	0.72	45	121.0	225.8	13.0	+	C/1946	P1	1.14	44	108.2	127.2	−19.7	−
C/1954	O2	3.87	42	53.6	336.6	−18.9	+	C/1954	Y1	4.08	39	232.9	314.2	−23.9	−
C/1979	M3	4.69	42	126.8	207.4	14.6	+	C/1950	K1	2.57	37	269.3	138.5	−43.4	−
C/1960	M1	4.27	40	164.0	221.2	−12.3	−	C/1976	U1	5.86	37	90.2	310.0	−30.8	−
C/1925	G1	1.11	40	151.7	238.7	10.9	+	C/1974	F1	3.01	36	10.2	140.5	22.1	−
C/1990	M1	2.68	40	164.5	172.0	−48.4	−	C/1948	T1	3.26	34	307.4	324.5	17.4	−
C/1925	F1	4.18	35	327.1	66.4	−41.2	+	C/1903	M1	0.33	33	92.8	320.7	−34.5	−
C/1948	E1	2.11	34	83.9	250.1	−38.3	+	C/1978	A1	5.61	33	167.3	142.9	−31.0	−
C/1987	W3	3.33	29	63.2	334.5	64.1	−	C/1993	K1	4.85	33	346.9	131.2	2.6	−
C/1913	Y1	1.10	29	238.4	282.6	−52.5	−	C/1989	X1	0.35	32	218.5	325.6	−41.4	−
C/1947	Y1	1.50	28	37.3	245.1	−49.1	+	C/1992	J1	3.01	28	0.9	316.8	−44.2	+
C/1906	E1	3.34	28	133.6	38.1	−44.9	−	C/1978	H1	1.14	24	29.6	124.9	−20.4	+
C/1914	M1	3.75	27	101.0	201.2	−0.8	−	C/1925	W1	1.57	24	140.7	323.9	−21.6	−
C/1902	R1	0.40	27	229.5	189.0	−16.9	−	C/1944	K2	2.23	18	158.6	125.0	−31.5	−
C/1980	E1	3.36	27	29.8	177.3	−17.6	+	C/1988	B1	5.03	13	122.8	316.1	−48.0	−
C/1902	X1	2.77	26	191.1	20.8	−31.0	−	C/1974	V1	6.02	11	63.7	309.5	27.6	−
C/1907	E1	2.05	25	280.6	53.4	−20.4	+	C/1946	C1	1.72	−13	277.7	312.6	−60.7	+
C/1962	C1	0.03	25	106.3	218.6	27.5	+	C/1983	O2	2.25	−18	178.4	134.2	−27.6	−
C/1947	S1	0.75	24	170.2	185.8	11.5	+	C/1978	G2	6.28	−23	260.2	126.9	−33.9	−
C/1975	E1	1.22	23	178.2	55.1	42.0	+	C/1899	E1	0.33	−109	264.1	308.5	50.5	+
C/1922	U1	2.26	21	53.0	271.2	16.4	−								
C/1984	W2	4.00	20	100.3	79.5	32.9	+								
C/1973	E1	0.14	20	46.6	207.8	17.6	−								
C/1935	Q1	4.04	19	115.9	248.5	12.1	+								
C/1921	E1	1.01	18	143.1	219.3	−59.0	−								
C/1956	F1	4.45	17	62.1	180.3	−24.8	+								
C/1916	G1	1.69	17	30.5	226.4	18.4	−								
C/1991	F2	1.52	16	344.4	90.0	29.6	−								
C/1942	C1	1.45	16	22.1	89.8	−17.3	+								
C/1978	R3	1.77	15	18.5	31.0	24.3	−								
C/1853	L1	0.31	12	344.5	223.6	34.9	−								
C/1896	V1	1.06	5	243.7	192.5	2.2	+								
C/1993	Q1	0.97	3	173.8	112.5	41.4	+								
C/1940	R2	0.37	1	88.5	42.1	−24.4	+								
C/1946	U1	2.41	−1	255.3	347.7	48.4	+								
C/1892	Q1	0.98	−27	105.1	72.1	−32.5	−								
C/1942	C2	4.11	−34	335.0	19.2	−25.1	+								
C/1932	M1	1.65	−56	76.7	250.7	−25.1	+								
C/1898	V1	2.28	−71	172.4	11.0	−11.5	−								
C/1991	Y1	0.64	−94	102.7	16.9	9.0	+								
C/1952	W1	0.78	−125	10.2	84.9	15.6	−								
C/1895	W1	0.19	−172	354.5	31.9	48.8	−								

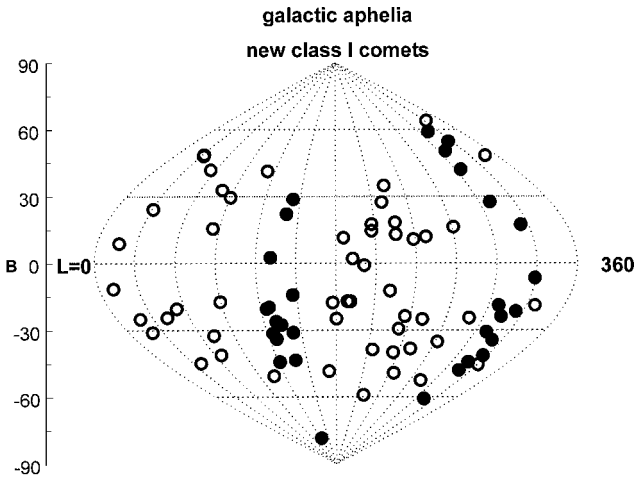

FIG. 1. Scatter of aphelia directions of 82 new class I comets in galactic coordinates.

In the next section we outline the dynamics of the relevant mechanisms. Following that we present in Section 3 several questions which could be raised when considering various features of the data. A statistical analysis emphasizing the significance of the correlations found is then given in Section 4. We end with a summary of our conclusions.

2. DYNAMICAL MECHANISMS

2.1. Stellar Impulse

In a strong stellar perturbation of the Oort cloud, impulses to both the Sun and the comets must be considered. The relative velocity will be typical of field stars. It has been shown (Weissman 1996) that in this case of a heavy shower, the distribution in aphelia directions will be nearly isotropic. Conversely, in a weak stellar perturbation of the Oort cloud we need only consider comet perturbations (Biermann *et al.* 1983) along an aphelia track that is relatively narrow and extends $<180^\circ$ across the sky.

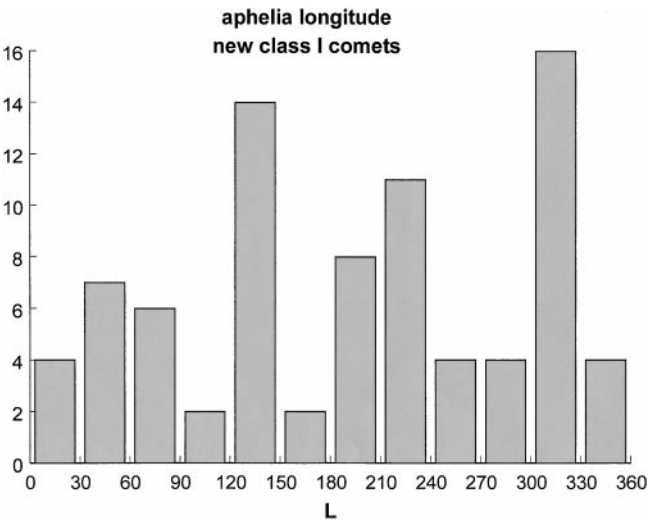

FIG. 2. Histogram of the aphelia longitude distribution of 82 new class I comets in galactic coordinates. A random distribution would be uniform in L.

2.2. Molecular Cloud Impulse

If the perturbation is due to a massive external perturber such as a molecular cloud, the tidal (differential) impulse on the comet–Sun system is appropriate. The anisotropic change in angular momentum is then given by (Bailey 1986)

$$\Delta\mathbf{H} \approx -\frac{GM_{\rm mc}R^2(\hat{\mathbf{n}}_U \sin 2\gamma_U + 2\hat{\mathbf{n}}_b \sin 2\gamma_b)}{U_{\rm mc} b_{\rm mc}^2}. \qquad (1)$$

Here $\mathbf{U}_{\rm mc}$ is the relative velocity between the cloud and the Sun, and $\mathbf{b}_{\rm mc}$ is the impact parameter. $\gamma_{U[b]}$ is the angle between the comet position vector $\mathbf{R}$ and $\mathbf{U}_{\rm mc}$ [$\mathbf{b}_{\rm mc}$]. The unit vectors are in the directions of $\mathbf{R}\times\mathbf{U}_{\rm mc}$ [$\mathbf{R}\times\mathbf{b}_{\rm mc}$].

2.3. Adiabatic Galactic Tide

The dynamics of the adiabatic galactic tide acting on near-parabolic Oort cloud comets is most simply given in a Newtonian framework (Matese and Whitmire 1996). It describes how the angular momentum and the perihelion distance ($H \approx \sqrt{2GM_\odot q}$, $\mathbf{H}\perp\mathbf{q}$) are changed by the galactic tide. Let $\mathbf{F}$ be the adiabatic galactic tidal force acting on a comet separated from the Sun by $\mathbf{R}=\mathbf{X}+\mathbf{Y}+\mathbf{Z}$. Here $\mathbf{X}$ points to the galactic core and $\mathbf{Z}$ points to the NGP. In the conventional approximation, at the solar location the galactic potential is taken to be azimuthally symmetric and the velocity curve is radially flat. The tidal force in a frame co-orbiting with the local matter (but with fixed axes) can then be modeled as (Heisler and Tremaine 1986) $\mathbf{F}=\Omega_\circ^2\mathbf{X}-\Omega_\circ^2\mathbf{Y}-\Omega_z^2\mathbf{Z}$, where $\Omega_\circ \equiv 2\pi/240$ Myr is the solar orbital frequency about the galactic core and $\Omega_z=\sqrt{4\pi G\langle\rho\rangle}$ is the nominal solar angular oscillation frequency about the galactic midplane. Here $\langle\rho\rangle$ is the azimuthal average of the local disk density (see Matese *et al.* (1995) for a discussion of modulated tidal forces due to time dependence in $\langle\rho\rangle$). The galactic tidal torque on the comet–Sun system is $\boldsymbol{\tau}=\dot{\mathbf{H}}=\mathbf{R}\times\mathbf{F}$.

For near-parabolic comets, $\mathbf{R}\approx R\hat{\mathbf{Q}}$, with cartesian aphelia unit vector components (more precisely antipodal directions to the observed perihelia vectors)

$$\hat{\mathbf{Q}} \approx \frac{\mathbf{Q}}{2A} = (\cos B\cos L, \cos B\sin L, \sin B). \qquad (2)$$

Secularly obtaining the change in angular momentum over an orbit period, P_A, we have

$$\Delta\mathbf{H}^{\rm tide} = \dot{\mathbf{H}}P_A = \frac{5}{2}P_A A^2\Omega_z^2\cos B \times[\hat{\phi}\sin B(1+\epsilon\cos 2L)+\hat{\theta}\epsilon\sin 2L], \qquad (3)$$

where $\hat{\phi},\hat{\theta}$ are the conventional spherical unit vectors in a

system of coordinates with radial direction $\hat{\mathbf{Q}}$. The *visible* values are $\langle\rho\rangle \approx 0.1\, M_\odot pc^{-3}$ and $\epsilon \equiv \Omega_\circ^2/\Omega_z^2 \approx 0.1$. Recent dynamically inferred values (Crézé *et al.* 1998) are consistent with that seen, but averages over many past independent dynamical studies suggest some compactly distributed dark disk matter (Stothers 1998).

Both components of $\dot{\mathbf{H}}$ are essentially constant over one orbit period:

$$\cos B\Delta L \approx \Delta B \approx \text{order}\left[\frac{\Delta H}{H}\frac{q}{A}\right].$$

In contrast, because $\mathbf{H}$ itself is rapidly changing, any formalism which evaluates

$$\begin{aligned}\dot{H} = H^{-1}(\mathbf{H}\cdot\dot{\mathbf{H}}) &= H^{-1}(H_\phi\dot{H}_\phi + H_\theta\dot{H}_\theta)\\ &\equiv -\cos\alpha\dot{H}_\phi - \sin\alpha\dot{H}_\theta \qquad (4)\end{aligned}$$

will find $\dot{H}$ caused by the galactic tide to be changing rapidly in the course of a single orbit. This highlights the value of the Newtonian presentation. In Table I, the columns labeled $\dot{H}$ give the signature of the osculating value of Eq. (4) evaluated at perihelion, and α is as defined in Eq. (4).

It is conventionally assumed that the *in situ* angular momentum distribution of new Oort cloud comets of specified semimajor axis A can be adequately approximated in this case by the loss cylinder model,

$$\frac{d^2N}{dH_\phi dH_\theta} \propto \Theta\left(H_\phi^2 + H_\theta^2 - H_{\rm lc}^2\right), \qquad (5)$$

where Θ is the unit step function and $H_{\rm lc} \equiv \sqrt{2GM_\odot q_{\rm lc}}$. Here $q_{\rm lc} \approx 15$ AU is the loss cylinder boundary. This is a statement that comets which leave the planetary region having $q < q_{\rm lc}$ will likely have experienced an energy impulse from the planets which will have removed them from the new Oort cloud population (Fernandez 1981). Figure 3a is a schematic illustration of how this step-function loss cylinder must be refilled by a perturbation in order to make comets observable. It is also generally assumed that the *in situ* distribution of aphelia directions is adequately represented as isotropic, independent of $\mathbf{H}$ and x.

2.4. Bound Perturber Impulse

We now consider the dynamics of a putative small-mass bound perturber interacting with a comet, assuming that the solar perturbation is negligible. The impact parameter is taken to be sufficiently small that the radial coordinates of both the comet, $\mathbf{R}$, and the perturber, $\mathbf{r}$, are nearly parallel. The perturber orbit is assumed to lie in the plane defined by the great circle. Symbol

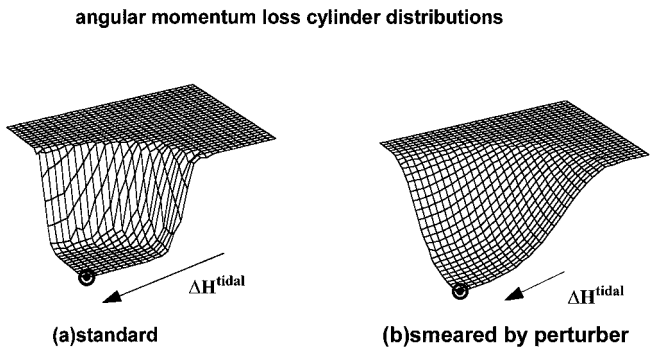

FIG. 3. Schematic illustration of the loss cylinder in angular momentum space. (a) In the absence of a bound perturber. (b) As smeared by a bound perturber.

notation is as follows:

Impact parameter:	$\mathbf{b} = (b_{\rm r}, b_\theta, b_\phi)$
Perturber position:	$\mathbf{r} = (r, 0, 0)$
Angular impact parameter:	$\beta \equiv \mathbf{b}/r$
Perturber velocity:	$\mathbf{v} \approx (v_r, v_\theta, 0)$
Perturber mass:	M
Comet position:	$\mathbf{R} \equiv \mathbf{r} + \mathbf{b}$
Comet velocity:	$\mathbf{V} \approx (V_{\rm r}, 0, 0)$
Comet angular momentum:	$\mathbf{H} \equiv \mathbf{R} \times \mathbf{V}$
Comet energy:	$\mathcal{E} \equiv -\frac{GM_\odot}{2A}$
Relative velocity:	$\mathbf{U} \equiv \mathbf{v} - \mathbf{V}$.

The velocity impulse to the comet is

$$\Delta\mathbf{V} = -\Delta\mathbf{U} = -\frac{2GM\mathbf{b}}{Ub^2}, \qquad (6)$$

where $\mathbf{b} \perp \mathbf{U}$. The angular momentum impulse is then

$$\Delta\mathbf{H}^{\rm impulse} = \mathbf{R}\times\Delta\mathbf{V} = \mathbf{r}\times\Delta\mathbf{V} = \frac{2GM}{U}\frac{\beta\times\hat{\mathbf{r}}}{\beta^2}, \qquad (7)$$

with components

$$\Delta H_\theta = \frac{2GM\beta_\phi}{U\beta^2}, \qquad \Delta H_\phi = -\frac{2GM\beta_\theta}{U\beta^2}. \qquad (8)$$

Scaling to the change required to bring comet perihelia from the edge of the loss cylinder to the center of the observable zone, we have

$$\frac{\Delta H}{H_{\rm lc}} = \frac{\Delta H}{(2GM_\odot q_{\rm lc})^{\frac{1}{2}}} \approx \pm\left(\frac{2r}{3q_{\rm lc}}\right)^{\frac{1}{2}}\frac{1}{\beta}\frac{M}{M_\odot}. \qquad (9)$$

Note that if there is an impulse which brings a comet into the observable zone, the fractional change in energy will be substantially smaller

$$\frac{\Delta\mathcal{E}}{\mathcal{E}} \approx \frac{V_{\rm r}\Delta V_{\rm r}}{\mathcal{E}} = -4\frac{V_{\rm r}}{U}\frac{A}{r}\frac{M}{M_\odot}\frac{\beta_{\rm r}}{\beta^2} \approx \pm\left(\frac{8}{3}\right)^{\frac{1}{2}}\frac{1}{\beta}\frac{M}{M_\odot}. \qquad (10)$$

In the approximations for the fractional changes we have adopted the following estimates, $r \approx A$, $\beta_r \approx \beta_\theta \approx \beta_\phi \approx \beta/\sqrt{3}$, $v_\theta \approx V_r \approx U/\sqrt{2} \approx \sqrt{GM_\odot/r}$.

Impulsed comets could be moving either inward or outward at the perturbation site. Therefore it is of interest to discuss the free fall time of a comet from R, A. We denote the mean anomaly of the perturber orbit $\mathbf{r}$, a, by $m(r) = \frac{2\pi}{P_a}(t - \tau_M)$. The free fall time of a near-parabolic comet from R is

$$t_{\rm ff}(R, A) = \frac{P_A}{2\pi}\left\{\pi + Sgn(\dot{R})\left[\frac{\pi}{2} - \sin^{-1}\left(\frac{R}{A} - 1\right) + \left(\frac{R}{A}\left(2 - \frac{R}{A}\right)\right)^{\frac{1}{2}}\right]\right\}. \quad (11)$$

Letting $t = 0 \equiv$ the present epoch and approximating $R \approx r$, we obtain the relation for the mean anomaly of the perturber when it impulsed a comet at a time $-t_{\rm ff}(R \approx r, A)$ in the past:

$$m(r) + \frac{2\pi\tau_M}{P_a} = -\frac{P_A}{P_a}\left\{\pi + Sgn(\dot{R})\left[\frac{\pi}{2} - \sin^{-1}\left(\frac{r}{A} - 1\right) + \left(\frac{r}{A}\left(2 - \frac{r}{A}\right)\right)^{\frac{1}{2}}\right]\right\}. \quad (12)$$

If we knew the complete set of orbital elements of the putative bound perturber, then Eq. (12) could be solved to determine the locus of possible values of cometary A simultaneously seen today around the great circle. The solution would be multivalued; i.e., at any point on the great circle we could be seeing comets that were freely falling inward when the perturber made its most recent passage, but we could also be seeing comets that were freely falling outward when the perturber impulsed them on one (or more) perturber orbits ago.

Having given an overview of the relevant dynamical relations, we now return to the data to inquire about the implications.

3. QUESTIONS RAISED BY THE OBSERVATIONS

3.1. Can the Longitude Distribution Be Caused by Any of These Mechanisms?

Of the dynamical themes discussed, we can reject the possibility that the great circle is produced by a strong field star impulse since such a perturbation produces a near-isotropic distribution of aphelia directions (Weissman 1996).

This does not mean that no observed new comets are attributable to a stellar impulse. Matese *et al.* (1998) concluded that the secondary peak centered at 225° was a residual part of a weak comet shower noted by Biermann *et al.* (1983). It is localized in a region ($L = 180°$–$240°$ and $B = 0°$–$30°$) that is weakly perturbed by the galactic tide. The shower is more strongly evidenced in energies $x > 100$, thus indicating that it is the temporal flux tail of a recent shower. The predicted pattern of a weak stellar impulse shower (a narrow track extending $<180°$) is consistent with the observed Biermann shower. Such a prediction leads us to conclude that the ≈270° great circle is not the product of a weak stellar impulse. This is the only substantive argument against a weak stellar shower interpretation of the great circle anomalies.

Can a molecular cloud impulse produce the great circle? The angular dependencies contained in the expression for the angular momentum change in Eq. (1) ($\sin 2\gamma$) are incapable of producing the narrow width in the observed longitude distribution for the great circle. Therefore we also reject a molecular cloud impulse as an explanation for the great circle.

In Fig. 2, we observe two large peaks (the great circle) and two secondary peaks in the longitude distribution. Does the core galactic tide play a role? Matese and Whitmire (1996) suggested this explanation. Subsequent studies (Matese *et al.* 1998) indicated that the appropriate quadrupolar terms ($\sin 2L$, $\cos 2L$) in Eq. (3) could not produce narrow longitude peaks unless one adopted an ad hoc *in situ* distribution of comet elements. The core tide as a major contributor can be rejected on this basis.

We are left with the adiabatic galactic disk tide and a putative bound perturber as potential dynamical explanations. The very nature of the longitude concentration of aphelia along an extended portion of a great circle suggests that it is a signature of the orbital path of a small-mass bound perturber. However, we shall see below that the latitude data bears the signature of the galactic disk tide.

3.2. Can the Latitude Distribution Discriminate between These Two Options?

In Fig. 4 we show a histogram of the galactic latitude distribution, distinguished between those comets in the great circle and those outside the great circle. It would be uniform in sin B

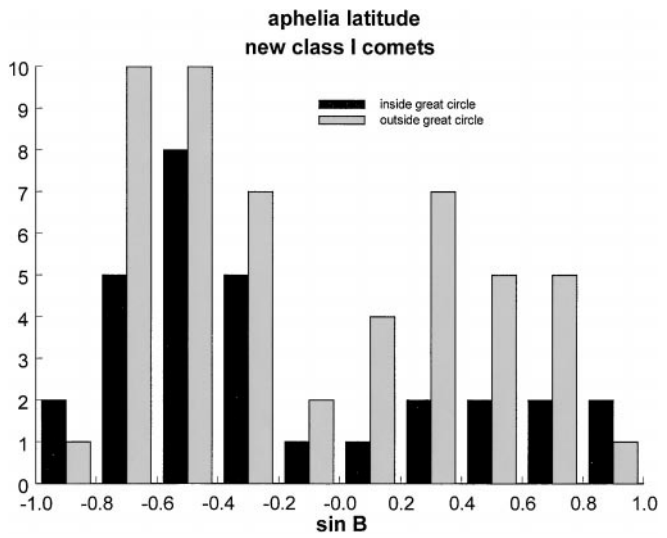

FIG. 4. Histograms of the aphelia latitude distributions of 82 new class I comets in galactic coordinates, separated as to inside and outside the "great circle." A random distribution would be uniform in sin B.

if observed aphelia were randomly scattered on the celestial sphere. Figure 1 shows that the definition of what constitutes the great circle band is somewhat arbitrary since there are some comets that visually could be incorporated but formally are not. We remark that inclusion of these comets would reinforce the conclusions we shall draw below.

Outside the great circle the aphelia latitude distribution exhibits signature deficiencies at the galactic poles and equator in both hemispheres. This results from the dominant disk tide for which $\Delta H_\phi \propto \sin B \cos B$. However, inside the great circle, something distinctive is seen. The southern galactic hemisphere distribution of aphelia has the prototypical shape, suggesting the galactic tide, but is overabundant by a factor of $\frac{21}{30}\frac{5}{1} = 3.5$. The northern galactic hemisphere distribution is overabundant by a more modest factor of 2 and is flatter with no clear signature of the tide, perhaps because of the small numbers involved. The hemispherical asymmetry is, in itself, of no clear statistical significance but it is curious.

Are either of the two dynamical mechanisms capable of explaining all of these conflicting results while maintaining a standard model for the *in situ* distributions of x and $\mathbf{H}$ and $\mathbf{Q}$? Do we have to abandon the assumption of *in situ* randomized distributions? To gain more insight we now look at the energy distribution.

3.3. *Can the Energy Distribution Help Us Discriminate?*

In Fig. 5 we show a histogram of the energy distribution, taken from Table I, distinguishing comets that are in and out of the great circle. It is noticed that there is a potential correlation with more tightly bound energies being associated with comets in the great circle. For energies $x < 30$ the great circle proportion exceeds what is expected for a random distribution by a modest factor of 1.5. However, for $x > 30$ the proportion exceeds random by a much larger factor of $\frac{20}{18}\frac{5}{1} = 5.5$. The statistical significance of this observation is discussed below. We need to explain (i) a great circle longitudinal excess which is (ii) disproportionately in tighter energies, and (iii) normal in displaying the latitude dependence signature of the galactic disk tide.

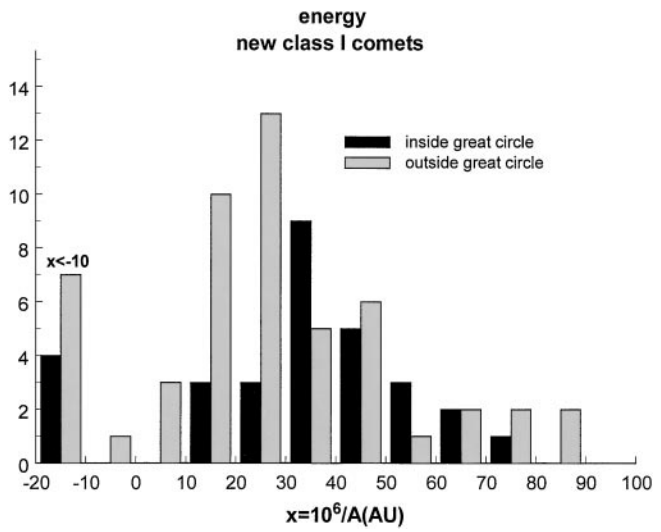

FIG. 5. Histograms of the energy distribution of 82 new class I comets, separated as to inside and outside the "great circle."

We believe the explanation for these apparently disparate bits of information is that one should *not* perceive the causal interaction to be *either* a bound perturber impulse *or* the galactic disk tide, *but both*.

The galactic tidal perturbation and the impulse should be superposed in the course of a cometary orbit. The tide changes the angular momentum from its prior value as the comet recedes from the planetary region and, after the perturber impulse, continues to change it until the comet enters the planetary region with its observed value:

$$\mathbf{H}^{\text{observed}} = \mathbf{H}^{\text{prior}} + \Delta\mathbf{H}^{\text{preimpulse-tide}} + \Delta\mathbf{H}^{\text{impulse}} + \Delta\mathbf{H}^{\text{postimpulse-tide}} \quad (13)$$

$$= (\mathbf{H}^{\text{prior}} + \Delta\mathbf{H}^{\text{impulse}}) + \Delta\mathbf{H}^{\text{complete-orbit-tide}}. \quad (14)$$

The simplest way to visualize this process is suggested by the bracketed terms in Eq. (14). Within a tube in space swept out by the perturber's "sphere of influence," all affected comets will effectively have their prior loss cylinder distribution smeared by the amount $\Delta\mathbf{H}^{\text{impulse}}$ given in Eq. (7). For these comets the standard step function for the prior distribution of angular momentum (Fig. 3a) is changed to a smeared distribution (Fig. 3b). The energy impulse was shown to be small, leaving the energy distribution essentially unaffected. Depending on the semimajor axes of those comets in the tube which are consistent with free-fall timing, Eq. (12), the outcome can roughly be categorized in one of three ways.

If A is sufficiently large, the bound perturber impulse is irrelevant since the tidal torque would be large enough to refill the loss cylinder anyway. No additional number of comets is made observable. Only the physical identity of the comets made observable is changed.

If A is sufficiently small, the galactic tide is irrelevant since the tidal torque is too small to be of significance. These observed comets can be considered to be directly injected by the perturber. This occurs if the impact parameter b (and therefore the cross section) is small. No latitude signature of the Galaxy is to be expected. These comets will provide an observed population in the tightly bound outer Oort cloud population not attributable to observational uncertainties or outgassing.

However if A is intermediate in value, the combined perturbation of the small-mass perturber and the galactic tide must be considered. With a loss cylinder boundary smeared inward (from the region of impact parameters b that is not small enough for direct injection into the observable zone), a weaker tide associated with an intermediate value of cometary semimajor axis A *can* be sufficient to make a comet observable. We should expect to see the galactic signature in the latitude distribution of this

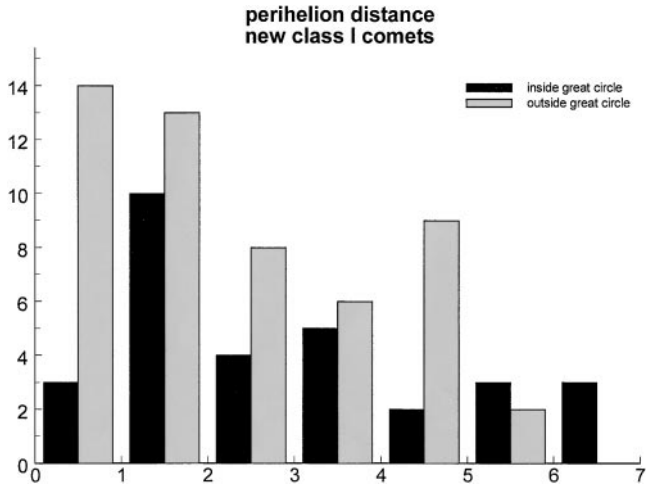

FIG. 6. Histograms of the perihelion distance distribution of 82 new class I comets, separated as to inside and outside the "great circle."

population, and we should expect to see an enhanced number of comets in the perturbed tube with intermediate values of A.

We therefore have a potential *dynamical* explanation for the observations that we see (i) a great circle longitudinal excess which is (ii) disproportionately in tighter energies and (iii) normal in displaying the signature latitude dependence of the galactic disk tide. Supporting evidence for this conjecture can be found in the perihelion distance distribution.

3.4. How Does the Perihelion Distribution Support the Conjecture?

In Fig. 6 we show the histogram of the perihelion distance distribution taken from Table I. We observe that for $q < 1$ AU the proportion of the in-circle and out-of-circle populations is nearly the random expectation of 1 to 5. The excess count in the great circle is strictly in larger perihelion distances. Why? We suggest that it is precisely because the combined effects of perturber impulse and disk tide are still sufficiently weak for the more numerous intermediate A comets that angular momentum changes will tend to barely enable the perihelion to move into the observable region as indicated in Fig. 3b. The statistical significance of this data is discussed in the next section.

Matese and Whitman (1992) have showed that there was a significant increase in the tidally produced observable comet flux when q_{lc} was decreased. This is effectively what occurs due to the perturber impulse.

3.5. Is There Any Other Supportive Evidence?

Consider Eqs. (3) and (4) showing the change in angular momentum due to the galactic tide. If the combined effects *were* barely sufficient to make the comet observable, then the osculating value of the galactic tidal $\dot{H}$ should be negative. Equation (4) has been evaluated and its signature recorded in Table I. Observe that there is indeed an excess of negative values in the great circle (the statistical significance of which is documented below) and that this excess tends to be correlated with the energy range $30 < x < 50$. We suggest that values $50 < x$ are either erroneous because of observational uncertainties or outgassing or are directly made observable by the perturber impulse. Values $x < 30$ may be erroneous because of observational uncertainties or outgassing, or may be dominated by the conventional tide for which angular momentum changes are so large that $\Delta\mathbf{H}$ is equally likely to overshoot or undershoot the center of the loss cylinder. Further evidence that the core tide is not the dominant dynamical mechanism here is the fact that the distribution in $\dot{H}$ is minimally changed when we set the core parameter $\epsilon = 0$.

3.6. What Is the Likely Orbit of the Perturber?

A fit of the great circle aphelia directions yields an inclination to the NGP of $88^\circ[92^\circ] \pm 3^\circ$. Since the sense of the perturber orbital motion is unknown, we adopt an inclination of $i = 90^\circ \pm 5^\circ$ for the perturber orbit normal.

We can get a rough estimate of the orbit size by returning to the prediction of the locus of energies along the great circle. *For simplicity of discussion* we consider a circular perturber orbit. Inserting $r = a$ into Eq. (12) we plot in Fig. 7 the phase of the perturber $m(r = a) + 2\pi\tau_M/P_a$ (expressed in orbit cycles) versus the ratio of semimajor axes a/A. For a circular perturber orbit, $a/A \leq 2$ if the perturber is to intersect the comet path. A phase value of zero corresponds to the present location of the perturber along the great circle (which is, of course, unknown). The rapidly rising part of the curve corresponds to comets that were

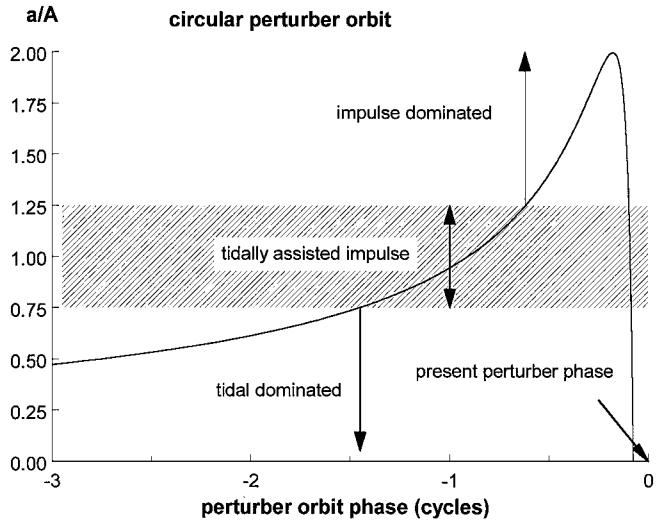

FIG. 7. The semimajor axes of simultaneously observable comets, A, expressed as a ratio to that of the perturber, a, for the special case of a circular perturber orbit. The ratio is plotted versus the angular orientation along the great circle, expressed in orbit cycles. Phase = 0 corresponds to the present (unknown) angular location of the perturber. The band illustrated is the region where the galactic tidal torque and the perturber impulse act in concert to make the comet observable. For a perturber semimajor axis of $a = 25{,}000$ AU, the ratio $a/A = x/40$.

freely falling directly inward when they were recently perturbed subsequent to their aphelion passage. The peak in the curve corresponds to the perturber impulsing comets at their aphelion ($r = a \approx Q \approx 2A$) slightly earlier in time. Still earlier in time the perturber impulsed comets on their way out to aphelion. We are simultaneously seeing comets from all phases (perturbation sites along the great circle), each corresponding to a different comet energy. However, the situation is yet more complicated by the fact that perturbed comets with sufficiently large A could continue on this orbit of the Sun for longer than one perturber period (when the perturber phase at comet impulse was <-1 cycle) before entering the planetary system. Therefore, at any angle along the great circle, there corresponds a discrete set of near-parabolic cometary energies which could be simultaneously seen. Analogous curves obtain for perturber orbits of any eccentricity and phase.

It is important to note that it would be impossible to simultaneously see comets if they were all impulsed near their aphelia in the great circle. Simultaneously observed comets must have been impulsed at different cometary orbital phases and must have a range of energies.

To estimate the perturber orbit radius, we take the interval $30 < x < 50$ to denote the energy range where the *combined* perturbation is important. Also estimating the angular arc of this region as $\approx 3/4$ of a perturber orbit cycle (270°), we find from Fig. 7 that $a/A \approx 1.00 \pm 0.25$. The range of larger ratios is impulse dominated and that of smaller ratios is tidal dominated.

Taking $\langle x \rangle \approx 40 \approx 10^6$ AU$/\langle r \rangle$, we obtain a preliminary estimate for the mean radius at the interaction sites along the arc of ≈25,000 AU. The perturber orbit may be more nearly circular than parabolic; i.e., $e^2 < 0.5$ is more likely than $e^2 > 0.5$. Note that the present phase of the perturber, defined as phase cycle = 0, is spatially equivalent to phase cycles -1, -2, etc.

A *hypothetical* illustration based on Figs. 1 and 7 is now presented. If the perturber were in a near-polar orbit and if it was presently located at $L = 315°$, $B = -60°$ (≡cycle 0), moving toward the NGP, the description of the observed perturbed comet population would be as follows. Any perturbed comets in the prior 0.1 cycle (≈35°) could not have made themselves observable today since the free fall time is too long. A very small group of comets recently perturbed near phase -0.1 as they freely fell inward could be observable and would be imbedded in a part of the arc at an equivalent phase of ≈ -1.1. These comets would be located near $L = 135°$, $B = -85°$, close to the SGP. However, since the tidal torque is so weak near the poles, we should not expect many comets in this small group to be made observable.

Directly injected (impulse dominated) comets could be seen at phases -0.1 to -0.65, trailing the perturber by ≈35° to 235° and extending up through the $L = 135°$ band, beyond the NGP, terminating in the $L = 315°$ band. Comets such as C/1959 X1, C/1898 L1, C/1987 F1, and C/1976 D2 might be in this class.

At perturber phases -0.65 to -1.45, covering an arc of ≈285°, which extends from $L = 315°$, $B = +65°$ to $L = 135°$, $B = +40°$, we have the dominant class of observed comets from the combined tidally assisted + perturber impulse interactions. The observed comet energies would *systematically* change from $x = 50$ to $x = 30$ as one proceeds along this portion of the arc. Gaps at the equator and poles would occur because of weakened tidal torques. All of these comets would have been perturbed at different times on their way out to aphelia but could now be simultaneously observed.

Still earlier perturber phases (<-1.45 cycles) would be associated with comets having $x < 30$ for which the tide would be dominant and would produce an observed population 1/5 of that outside the great circle. The hemispherical nonuniformity in the observed distribution along the great circle could be due to the dynamics of free fall embodied in Eq. (12) or could be due to eccentricity in the perturber orbit.

Unfortunately, the original energy determinations are sufficiently inaccurate due to observational uncertainties and outgassing effects that we cannot use such an analysis as presented above to predict the perturber location, sense of motion, or eccentricity, so we should not attempt to push this crude picture too far. Analogous curves have been obtained for more general orbits having larger eccentricities.

3.7. What Determines the Width of the Arc and the Perturber Mass?

Equation (9) provides the information. The angular width of the observed great circle is $\beta \approx 0.2$ radians. We argue that the angular momentum impulse due to the perturber must be of the order of the loss cylinder dimension, H_{lc}, inside the great circle tube. Inserting q_{lc} as well as the estimate of $\langle r \rangle$ at the interaction site, and taking $\Delta H / H_{lc} \approx 1/2$, we obtain $M \approx 0.003 M_\odot$. That is, the angular width is 0.2 radians because the perturber mass is $\approx 3 M_J$. Taking into account the uncertainties in the parameter estimates, we suggest a range of $3 \overset{\times}{\div} 2 M_J$.

3.8. What Limits the Mean Perturber Radius?

Hills (1985) has shown that objects in the Oort cloud more massive than $0.01 M_\odot$ would refill the loss cylinder due to direct impulses. If the perturber mass was close to $0.01 M_\odot$ and it was in an orbit which could perturb comets with $A \leq 30{,}000$ AU the signal would be sufficiently strong as to dominate the galactic tide. This is true independent of perturber eccentricity and inclination. However, if the mass is closer to $0.003 M_\odot$, then we are on the borderline of detectability since the cross section is $\propto M^2$.

We have demonstrated that objects down to $0.003 M_\odot$ could partially refill the observable part of the loss cylinder and would be more effective with the aid of the galactic tide. The assistance of the galactic tide requires $A \geq 20{,}000$ AU. If the perturber mass was as little as $0.003 M_\odot$, and it was in an orbit which could perturb comets with $A \leq 20{,}000$ AU, the loss cylinder would be partly refilled with directly injected comets. Since the *in situ* flux of comets increases approximately as $A^{-5/2}$ we would see

a large number of directly injected comets with $A \approx 10{,}000$ AU. The absence of such an observed population suggests a lower limit for $\langle r \rangle$.

Conversely if the perturber was in an orbit which could perturb comets with $A > 30{,}000$ AU, the galactic tide would not need the assistance of the impulse since it would already completely refill the loss cylinder. This suggests an upper limit for $\langle r \rangle$. Thus we have estimated the *mean* perturber radius over the $\approx 270^\circ$ arc to be $\approx 25{,}000$ AU.

3.9. What Explains the Amount of Excess in the Great Circle?

The *in situ* flux of new comets, differential in energy, and angular momentum is represented by

$$\frac{d^3\dot{N}(in\ situ)}{d\mathbf{H}\,dx} = \frac{1}{P_A}\frac{d\mathcal{P}}{d\mathbf{H}}\frac{dN}{dx}, \tag{15}$$

where

$$\frac{d\mathcal{P}}{d\mathbf{H}} = \frac{\Theta(H - H_{\rm lc})}{\pi\left(H_{\rm max}^2 - H_{\rm lc}^2\right)} \approx \frac{\Theta(H - H_{\rm lc})}{\pi G M_\odot A} \tag{16}$$

is the *in situ* angular momentum probability density and $\frac{dN}{dx}$ is the *in situ* energy number density. The differential flux of comets impulsed by the perturber is

$$\frac{d^3\dot{N}(\text{impulsed})}{d\mathbf{H}\,dx} = \int d\mathbf{H}_{\rm o}\frac{d\mathcal{P}}{d\mathbf{H}_{\rm o}}\frac{d\Sigma(\mathbf{H}_{\rm o}\to\mathbf{H})}{d\mathbf{H}}U\frac{dn}{dx}, \tag{17}$$

where $\frac{d\Sigma(\mathbf{H}_{\rm o}\to\mathbf{H})}{d\mathbf{H}}$ is the differential cross section for impulsing comets $\mathbf{H}_{\rm o}$ into $\mathbf{H} = \mathbf{H}_{\rm o} + \Delta\mathbf{H}^{\rm impulse}$. The *in situ* energy density per unit volume is

$$\frac{dn}{dx} = \frac{1}{2\pi R^2 P_A V_{\rm r}}\frac{dN}{dx}. \tag{18}$$

Comparing Eqs. (15) and (17) we can contrast the conventional loss cylinder distribution with the impulse-smeared distribution within the great circle tube of cross section $\Sigma \approx \pi b^2$,

$$\Theta(H - H_{\rm lc}) \leftrightarrow \int_{H_{\rm o} > H_{\rm lc}} d\mathbf{H}_{\rm o}\frac{d\Sigma(\mathbf{H}_{\rm o}\to\mathbf{H})}{d\mathbf{H}}\frac{U}{2\pi R^2 V_{\rm r}}. \tag{19}$$

Both the *in situ* and the impulsed fluxes are assumed to have a power law energy distribution $\frac{1}{AP_A}\frac{dN}{dx} \propto x^k$, where $k \approx 2.5$–4.5 (Bailey 1986). The galactic disk tide is assumed to refill the loss cylinder for $x < 30$, whereas the combined perturber plus tidal interaction is assumed to partially refill the loss cylinder for $30 < x < 50$. Therefore, our estimate for the energy integrated ratio is

$$\frac{\dot{N}(\text{perturber assisted})}{\dot{N}(\text{tide alone})} \approx \frac{\pi b^2 U}{2\pi R^2 V_{\rm r}}\frac{50^{k+1} - 30^{k+1}}{30^{k+1}}. \tag{20}$$

Setting $b/R = \beta = 0.2$, $U = \sqrt{2}V_{\rm r}$, $k = 3.5$ we obtain a ratio of 0.25.

Of the 82 new class I comets, Matese *et al.* (1998) estimate that <10% are associated with the temporal tail of the Biermann shower. For the 20 excess comets in the great circle, we now estimate that ≤5 would be tightly bound comets directly injected into the observable zone by the perturber. Therefore the comparable "observed" ratio would be $\approx 20/62 = 0.32$, which is in reasonable agreement with the theoretical estimate.

3.10. Is the Great Circle Excess Seen in Other Energy Populations?

No it is not (Matese *et al.* 1998). The great circle overpopulation is absent in both the new class II and the young ($100 < x < 1000$) populations. This presents a difficulty with most dynamical explanations of the great circle. If we *were* observing the onset of a weak stellar shower, one could explain the absence of a significant associated young overpopulation as being due to a lack of time for the planets to process the new population into a young one. This is the other extreme of the scenario used to explain the Biermann shower. However, as we have argued, a weak stellar shower will be seen along a celestial arc extending <180° and could not explain the observed arc of ≈270°.

We suggest that the fading of comets may play a role here. Young comets are less likely to be found at large perihelion distances than are new comets (Wiegert and Tremaine 1999). Since new class I great circle comets preferentially have large perihelia, they are more susceptible to fading from view on subsequent passages through the planetary region and would be less likely to subsequently appear in the young population. If the present conjecture is found to be correct, significant insights into the fading problem are possible.

3.11. Why Is the Orbit Near-Polar?

Perhaps it is because we would not have noted the signal in longitude distributions if the orbit was oriented otherwise. Matese *et al.* (1998) did analyze longitude distributions in ecliptic and equatorial coordinates as well as in galactic coordinates and could have detected anomalous great circle concentrations in any of these frames. Concentrations in longitudinal distributions of the amount seen here would likely be noticed if the great circle were inclined by as much as 10°. The probability that a randomly aligned great circle passes within 10° of the poles is $\sin(10^\circ) = 0.17$. Taking account of the fact that analogously oriented anomalous concentrations would have been seen in either ecliptic and equatorial coordinates, we are not unusually fortunate to have such an orbit orientation. We do not claim that the perturber has been in this orbit for any extended amount of time. Any orbit in the outer Oort cloud is liable to be substantively perturbed over hundred-Myr time scales (Hills 1985).

The galactic tide *does* provide a mechanism for *correlating* near-circular and near-polar orbits. The galactic tide will change the angular momentum of the *perturber* orbit as well as that of comet orbits. The z component of the perturber angular momentum, $H_z = H\cos i$, is nearly conserved with the core galactic tide

imparting an oscillation of small amplitude. If we neglect this effect, invariant (stable) orbits under the galactic disk tide fall into two classes (labeled "case (a)" and "case (e)" in Matese and Whitman (1989)). Neither stable orbit family includes a polar orbit (see also Breiter *et al.* (1996) who gave an extended discussion of possible orbital characteristics).

In fact, a circular orbit through the galactic poles is an *unstable* equilibrium configuration ("case (c)" in Matese and Whitman; also discussed in Breiter *et al.*). This is not a serious objection to the present conjectured orbit. Under the action of the galactic tide, such an orbit would undergo periodic osculations of period $P_{\rm H} \propto P_z^2/P_a$ where $P_z \approx 60$–90 Myr is the nominal solar oscillation period about the galactic midplane. Osculation periods exceeding hundreds of Myr are likely. Using the analysis presented there, we find that the predicted maximum eccentricity is related to the present elements by

$$1 - e_{\rm max}^2 = \frac{5}{4}(1 - e^2)\cos^2 i, \tag{21}$$

from which we determine $0.995 < e_{\rm max} < 1$ and $q_{\rm min} < 125$ AU for the perturber orbit.

That is, under the action of the galactic tide (and assuming no intervening impulses to the perturber, an unlikely event) the perturber would pass relatively close to the planetary zone every several hundred Myr, comparable to the time scales for strong field star impulses to the Oort cloud which would randomize their orbital parameters and substantively affect the perturber orbit. Hills (1985) has determined that objects of mass $<10 M_{\rm J}$ would not damage planetary orbits even if they had *passed through* the planetary system.

Further, in the course of a single osculation, the orbit will spend *more time* in the near-polar crossing, near-circular configuration than in its alternative extreme of a near-parabolic orbit. This is analogous (mathematically and figuratively) to a simple pendulum that can nearly reach its unstable equilibrium point. In the course of its oscillations, the pendulum will spend significantly more time near the unstable vertically up orientation than near the stable vertically down orientation.

Conceivably there are several jovian mass objects in the Oort cloud but this perturber is the one we are most likely to observe. Somewhat smaller objects could presently exist but they would not leave a notable imprint on comet distributions.

3.12. What Is the Likely Origin of the Perturber?

Extrasolar planets with masses $\sim 3 M_{\rm J}$ have been detected around several solar type stars at distances less than 5 AU (Fischer *et al.* 1999). In cases where there is significant eccentricity it has been suggested that these objects are brown dwarfs and therefore formed like stars rather than planets. Alternatively, the eccentricity could be the result of interactions between two massive extrasolar planets, in which case the less massive object would currently have a much larger orbit or would have been ejected from the system. The Oort cloud perturber under consideration here probably did not form like a jovian planet in the solar protoplanetary nebula since there is no mechanism for it to evolve by interactions with the known planets to its current outer Oort cloud orbit.

It is more likely that if a bound Oort cloud perturber exists it formed in a manner similar to the secondaries in wide binary systems. Hartigan *et al.* (1994) studied PMS wide binaries with projected separations between 400 and 6000 AU. They found that in 1/3 of the systems studied the secondary was systematically younger that the primary. This could be explained by capture if the less massive stars formed later than the more massive stars in the Taurus star forming complex studied. Alternatively the less massive star forms from a fragment independent of the primary (Pringle 1989). In this picture the secondary would accrete material more slowly than the more massive primary and therefore appear to be the younger of the pair (Hartigan *et al.* 1994). The Oort cloud perturber could have accreted at a few thousand AU and subsequently evolved to its current mean distance of 25,000 AU as the result of stellar impulses over 4.5 Gyr. The minimum brown dwarf mass based on Jeans instability considerations is $\sim 7 M_{\rm J}$ (Bodenheimer 1996). This is reasonably compatible with our nominal Oort cloud perturber mass estimate of $3 \stackrel{\times}{\div} 2 M_{\rm J}$.

3.13. Is This Brown Dwarf Observable?

The bolometric luminosity of a $3 M_{\rm J}$ jovian planet or brown dwarf is $\sim 6 \times 10^{-9} L_\odot$ if it is 5 Gyr old. Its effective temperature is $\approx$130 K, but its spectrum is orders of magnitude different than that of a blackbody in the wavelength range 1–10 μm (Burrows *et al.* 1997). Such an object at $\approx$25,000 AU would not have been observed by the IRAS survey but will easily be within the detection limits of SIRTF IR bands (Burrows *et al.* 1997). Depending on its mass, the perturber would also be within the detection limits of ISO and Gemini/SOFIA bands. It is also possible that its radio emissions would make it distinguishable in sensitive radio telescopes such as the VLA (Dulk *et al.* 1997). The perturber parallax angle would be $\approx$9 arcsec, significantly greater than its proper motion of $\approx$0.3 arcsec.

4. STATISTICAL ANALYSIS

We now discuss the statistical significance of the observations made in Section 3. The basic approach we take is to investigate hypothesized models of the distributions of the orbital elements and compare them with observations. Subjecting the comparisons to statistical tests we can determine p values, or significance levels. If $0.05 < p$, the observations are said to be consistent with the model and the hypothesis is regarded as reasonable. Values $0.01 < p < 0.05$ imply that there is some evidence against the assumed model, while $p < 0.01$ suggests that there is strong evidence against the model (McPherson 1990). Interpretational ambiguities can occur when different tests yield substantively different significance levels.

4.1. Does the Galactic Tide Really Dominate?

The data conventionally refered to as evidence that the galactic tide dominates in making Oort cloud comets observable during

the present epoch includes the latitude distribution illustrated in Figs. 1 and 4. This has been supported by analysis, and we review and augment those claims here.

A comparison of the observed distributions of *all* angular orbital elements to a hypothesized random distribution using a Kolmogorov–Smirnov (K-S) test of cumulative distributions has been performed (Matese and Whitman 1992). It was found that one could reject the hypothesis that the observed latitude distribution was a sample from a random distribution at a significance level $p < 0.05$. The significance level for rejecting the hypothesis that the observed latitude distribution was sampled from a random *in situ* population made observable by the galactic tide was only minimally larger even though the observed distribution visually favors the $|\sin B \cos B|$ profile over a random profile. This is likely to be a reflection of the inability of the cumulative K-S test to adequately discriminate here. The hypothesis that the observed distributions were samples from a random distribution *did* fail the K-S test at the level $p \leq 0.05$ for more independent dynamical variables than did the corresponding comparison with the galactic hypothesis.

In a χ^2 test of *binned distributions* (Matese *et al.* 1998) it was found that the hypothesis of a random distribution in both galactic latitude and longitude could be rejected at a significance level $p < 0.001$. When the tests were performed in ecliptic and equatorial coordinates it is found that $p > 0.05$ in all cases. The appropriate interpretation of these results is that there is suggestive evidence to reject the hypothesis of an observed random distribution of aphelia directions and that any nonrandomness is correlated in a way that points to the galactic coordinate system. Observational selection effects, stellar showers, and measurement errors were rejected as potential explanations for these results.

The strongest evidence that the galactic tide dominates today is the *association* between variables that is predicted by galactic tidal theory. We present statistical evidence for that here. In Eqs. (3) and (4) we see that perihelia distances will be decreased if $\langle \dot{H} \rangle < 0$ when averaged over an orbit

$$\Delta\sqrt{q} = \sqrt{q} - \sqrt{q_{\text{prior}}} \propto P_{\text{A}} \langle \dot{H} \rangle \propto A^{7/2}\, Sgn(\langle \dot{H} \rangle). \quad (22)$$

In the galactic tidal model, decreases in q are smallest for small negative $\langle \dot{H} \rangle$. Theoretically, small $\langle \dot{H} \rangle$ correlates with small A (large x), and small negative $\langle \dot{H} \rangle$ correlates with a negative observed (i.e., *osculating*) value of $\dot{H}$. Thus if x is large, the tide is weakened and large-x comets that are just barely made observable should have large q and an osculating value of $Sgn(\dot{H}) = -1$. Therefore galactic tidal theory predicts that there should be a correlation between $q - x$ and anti-correlations between $q - Sgn(\dot{H})$ and $x - Sgn(\dot{H})$. This is clear from the theoretical analysis and has been verified in model Monte-Carlo calculations including the galactic tide. They apply whether or not there exists a bound perturber partially aiding the galactic tide. The Monte-Carlo correlation results have been found to become more significant when one reduces the loss cylinder perihelion distance from the nominal value of 15 AU, moving it closer to the observed zone.

We have performed a conventional Kendall rank correlation test on these variables (Mathematica 1996, McPherson 1990). The $N = 82$ values of q, x, and $Sgn(\dot{H})$ in Table I are separately ranked from smallest to largest with ties treated in the prescribed fashion. We use the conservative Kendall ranking procedure rather than the more common Pearson test (which directly uses values in the correlation analysis) so that unreliably extreme values of x do not unduly bias the results. Values of q and $Sgn(\dot{H})$ are accurately known. Kendall's correlation coefficient, τ, is approximately normally distributed with zero expectation value and variance $\frac{4N+10}{9N(N-1)} = (0.0752)^2$ if the two variables have no correlation.

The results are $\tau(q, x) = 0.171$, $\tau(q, Sgn(\dot{H})) = -0.133$, and $\tau(x, Sgn(\dot{H})) = -0.081$. The corresponding one-sided p values are, respectively, $p = 0.011$, 0.039, and 0.14. That is, if q and x were truly unassociated, the probability that they would be positively correlated at this level or greater is 0.011, so we have some evidence that we can reject the hypothesis that the observed orbital elements are unassociated as is assumed in a random distribution model. Conversely we cannot reject the hypothesis of the galactic tidal model, which predicts such associations.

Further, the probability that all three correlations/anti-correlations predicted by the galactic tidal model would simultaneously occur at this level or greater if the elements were mutually unassociated is obtained in the Fisher method by evaluating

$$\chi^2 = -2 \ln[p(q, x)\ p(q, Sgn(\dot{H}))\ p(x, Sgn(\dot{H}))] = 19.4, \quad (23)$$

which is distributed like a χ^2 distribution with 3×2 degrees of freedom. The convolved p value is $p_{\text{combined}} = 0.0035$. The significance level of this correlation result is the best evidence that today Oort cloud comets are predominantly made observable by the galactic tide. It is essential that these correlations be firmly established before we discuss whether the great circle sample is anomalous.

4.2. Is the Overpopulation of the Perceived Great Circle Significant?

If we randomly scatter 82 points on a the celestial sphere, the probability that we would find ≥ 30 points in a single prechosen region of solid angle $4\pi/6$ steradians is found to be 1.1×10^{-5}. However, *a priori* we have no basis for choosing either the width, the inclination, or the phasing of the region. It is evident from Fig. 1 that the properties of the great circle band discussed here will nearly optimize this statistic, so it must be appropriately interpreted. In Sections 3.7–3.9 we see that the size and overpopulation of the band is largely determined by the mean radius at perturbation and the mass of the perturber, which we estimate to be $\langle r \rangle \approx 25{,}000$ AU and $M \approx 0.003 M_{\odot}$. The unknown orientation of the perturber plane is inferred from the orientation of the perceived great circle of comet aphelia. Should the conjectured perturber be discovered with the inferred properties, the

statistical and dynamical arguments presented would leave little doubt that it was the cause of the modest overpopulation.

An anonymous referee has scattered 82 points on the celestial sphere having a probability distribution $\propto |\sin B \cos B|$ and finds that an arbitrarily phased and inclined great circular band of $4\pi/6$ steradians containing ≥ 30 points occurs with probability 0.025. This is not small enough to convincingly argue that we have strong evidence to reject the hypothesis that the observed population is a sample from a distribution predicted by the conventional longitudinally symmetric galactic disk model, absent any additional dynamical mechanism. The conclusion is reasonable, but standard interpretations indicate that there is *some* evidence for rejecting this hypothesis, which justifies further investigation.

If the only observation was a great circle band consistent in size and overpopulation with the conjectured perturber, the present hypothesis would not be solidly based. However, that is *not* the case as we now show.

4.3. Correlations of Orbital Parameters with Longitude

In Section 4.1 we found that the mutual correlations, large x–large q–negative $Sgn(\dot{H})$, are predicted by galactic tidal model calculations and that these predicted correlations increase when the separation between the loss cylinder and the observable zone boundaries is reduced. When the loss cylinder boundary is effectively reduced because of smearing due to a perturber, proportionally more comets would be observed with intermediate values of A ($30 < x < 50$) since the reduced interval between the boundaries enables intermediate-A comets to be made observable by the galactic disk tide. This in turn would cause an even tighter association between large x, large q, and negative $Sgn(\dot{H})$. Therefore when we perform a Kendall rank correlation test between x, q, $Sgn(\dot{H})$, and galactic longitude L, we test the present perturber hypothesis.

For all 82 comets in Table I we have assigned a rank of $I_L \equiv -1$ if the comet was outside the great circle, and $I_L \equiv +1$ if it was inside the great circle. The correlation results are $\tau(x, I_L) = 0.151$, $\tau(q, I_L) = 0.129$, and $\tau(Sgn(\dot{H}), I_L) = -0.280$. With a standard deviation of 0.0752, the respective one-sided p values are $p = 0.023$, 0.043, and 0.0001, respectively. Therefore we conclude that the results indicate that there is significant evidence, both marginal and strong, that these characteristic signatures of the galactic tide are more strongly associated with comets inside the great circle than with comets outside the great circle. All three results are consistent with the prediction of a loss cylinder boundary that is effectively reduced by a bound perturber inside the great circle. Since x, q, and $Sgn(\dot{H})$ are themselves associated in the standard galactic tidal model, we cannot convolve these p values as in the application of the Fisher method above.

5. SUMMARY

We give strong evidence that there is a correlated set of anomalies in the distributions of orbital elements of new Oort cloud comets. The correlations include aphelia directions, energies, perihelion distances, and signatures of the angular momentum change due to the Galaxy. Aphelia directions of these comets form a "great circle" on the celestial sphere. It has previously been concluded that these anomalies are not likely to be attributable to observational uncertainties or selection effects. We have demonstrated that a bound low-mass brown dwarf perturber could provide a dynamical basis for the correlated observations.

Summarizing the statistical analysis, we argue that the combination of a modestly overpopulated great circle band with comet parameters that are unambiguously correlated in a statistically significant manner gives a sufficient basis for concluding that the present conjecture should be investigated observationally.

A substantive problem with the present conjecture is the absence of a comparable signal in the population of young comets having energies $100 < x < 1000$. However, as such, this problem may lead to new insights into the dependence of cometary fading on perihelion distance.

In all other regards, the data appear to be consistent with a model in which a perturber of mass $\approx 3 M_J$, having a mean distance at perturbation of $\approx$25,000 AU, helps to make these great circle comets observable, with the assistance of the galactic tide. It is possible that radio emissions from the brown dwarf would be distinguishable in sensitive radio telescopes such as the VLA. This object would not have been detected in the IRAS database, but will be detectable in the next generation of planet/brown dwarf searches, including SIRTF.

Even though the number involved is modest, $\approx$20 of 82 new comets, we remind the reader that Oort (1950) correctly inferred the existence of the comet cloud from a comparable population.

ACKNOWLEDGMENTS

The comments of Dr. Charles Anderson regarding the statistical analyses were helpful. Thanks also go to the Computational Astrophysics class for checking these results. J.J.M. and D.P.W. acknowledge the long-term contributions and intellectual stimulation provided by our friend and colleague Patrick G. Whitman, who died shortly before the completion of the manuscript.

REFERENCES

Bailey, M. E. 1986. The mean energy transfer rate to comets in the Oort cloud and implications for cometary origins. *Mon. Not. R. Astron. Soc.* **218**, 1–30.

Biermann L., W. F. Huebbner, and R. Lüst 1983. Aphelion clustering of "new" comets: Star tracks through Oort's cloud *Proc. Natl. Acad. Sci. USA* **80**, 5151–5155.

Bodenheimer, P. 1996. Formation of brown dwarfs and giant planets. In *Workshop on Planetary Formation in Binary Environment*, Stony Brook, NY. [abstract http://www.usr.obspm.fr/department/darc/planets/papers/stony-abs.html]

Breiter, S., P. A. Dybczynski, and A. Elipe 1996. The action of the galactic disk on the Oort cloud comets; Qualitative study. *Astron. Astrophys.* **315**, 618–624.

Burrows, A., M. Marley, W. B. Hubbard, J. I. Lunine, T. Guillot, D. Saumon, R. Freedman, D. Sudarsky, and C. Sharp 1997. A nongray theory of extrasolar giant planets and brown dwarfs. *Astrophys. J.* **491**, 856–875.

Byl, J. 1983. Galactic perturbations on nearly parabolic comet orbits. *Moon Planets* **29**, 121–137.

Crézé, M., E. Chereul, and C. Pichon 1998. The distribution of nearby stars in phase space mapped by Hipparcos. I. The potential well and local dynamical mass. *Astron. Astrophys.* **329**, 920–932.

Dulk, G. A., Y. LeBlanc, and T. S. Bastian 1997. Search for cyclotron-maser radio emission from extrasolar planets. In *29th DPS Meeting*. [abstract 28.03]

Fernandez J. 1981. New and evolved comets in the Solar System. *Astron. Astrophys.* **96**, 26–35.

Fischer, D. A., D. W. Marcy, R. P. Butler, S. S. Vogt, and K. Apps 1999. Planetary companions around two solar-type stars. *Publ. Astron. Soc. Pac.* **111**, 50–56.

Hartigan, P. K., M. Strom, and S. E. Strom 1994. Are wide pre-main sequence binaries coeval? *Astrophys. J.* **427**, 961–977.

Heisler, J. 1990. Monte Carlo simulations of the Oort comet cloud. *Icarus* **88**, 104–121.

Heisler, J., and S. Tremaine 1986. Influence of the galactic tidal field on the Oort cloud. *Icarus* **65**, 13–26.

Hills, J. G. 1985. The passage of a Nemesis-like object through the planetary system. *Astron. J.* **90**, 1876–1882.

Marsden, B. G., and G. V. Williams 1996. *Catalogue of Cometary Orbits*, 11th ed. Smithsonian Astrophysical Observatory, Cambridge.

Matese, J. J., and P. G. Whitman 1989. The galactic disk tidal field and the nonrandom distribution of observed Oort cloud comets. *Icarus* **82**, 389–401.

Matese, J. J., and P. G. Whitman 1992. A model of the galactic tidal interaction with the Oort comet cloud. *Celest. Mech. Dynam. Astron.* **54**, 13–36.

Matese, J. J., and D. P. Whitmire 1996. Tidal imprint of distant galactic matter on the Oort comet cloud. *Astrophys. J.* **472**, L41–43.

Matese, J. J., P. G. Whitman, K. A. Innanen, and M. J. Valtonen 1995. Periodic modulation of the Oort cloud comet flux by the adiabatically changing galactic tide. *Icarus* **116**, 255–268.

Matese, J. J., P. G. Whitman, and D. P. Whitmire 1998. Oort cloud comet perihelion asymmetries: Galactic tide, shower or observational bias? *Celest. Mech. Dynam. Astron.* **69**, 77–88.

McPherson G. 1990. *Statistics in Scientific Investigation*, pp. 484–488. Springer-Verlag, New York.

Oort, J. H. 1950. The structure of the cloud of comets surrounding the Solar System, and a hypothesis concerning its structure. *Bull. Astron. Inst. Neth.* **11**, 91–110.

Pringle, J. E. 1989. On the formation of binary stars. *Mon. Not. R. Astron. Soc.* **239**, 361–370.

Stothers, R. B. 1998. Galactic disc dark matter, terrestrial impact cratering and the law of large numbers. *Mon. Not. R. Astron. Soc.* **300**, 1098–1104.

Weissman, P. R. 1996. Star passages through the Oort cloud. *Earth Moon Planets* **72**, 25–30.

Wiegert, P., and S. Tremaine 1999. The evolution of long-period comets. *Icarus* **137**, 84–122.

Wolfram Research 1996. *Mathematica 3.0—Standard Add-on Packages*, p. 450. Cambridge Univ. Press, Cambridge, UK.